Indian Journal of Pure & Applied Physics
Vol. 58, December 2020, pp. 847-857

Synthesis and spectral analysis of (S)-7-(4-chlorophenyl)-6,7-dihydrothiazolo [4,5-d]pyrimidine-2,5(3H,4H)-dione and study of its quantum chemical properties

Huda Parveen[a], Abha Bishnoi*[a], Aaherasha Iqbal[b], Nishat Afza[a] & Sonam Rai[a]

[a]Department of Chemistry, University of Lucknow, Lucknow 226 007, India.
[b]Department of Chemistry, MTG Learning, Gurgaon, India.

Received 7 March 2020; accepted 15 October 2020

In this article, synthesis and quantum chemical properties of novel (S)-7-(4-chlorophenyl)-6,7-dihydrothiazolo[4,5-d]pyrimidine-2,5(3H,4H)-dione (CPTHZ) are described. The aim of this synthesis was to obtain biologically active thiazolidinone scaffolds and correlates its quantum chemical properties with its experimental results. The structure of the compound was characterized by using different spectral analysis. The chemical calculations were computed with the help of DFT level of theory using Becke3–Lee–Yang–Parr (B3LYP)) and Coulomb–Attenuated–Method–Becke3–Lee–Yang–Parr (CAM-B3LYP)/6-31G(d,p) basis set. Thermodynamic properties were calculated at diverse temperatures. Various structural and thermodynamic parameters such as electrophilicity, chemical potential, chemical hardness and maximum amount of electronic charge transfer were done for this compound. The local reactivity descriptors showed that most reactive site for nucleophilic attack was C(7). In addition to it, correlation graphs between experimental and calculated values of ^{1}HNMR and ^{13}CNMR were also presented.

Keywords: Density functional theory (DFT), dipole moment, hyperpolarizability, reactivity descriptor.

1 Introduction

Thiazolidin-4-one derivatives are known to exhibit diverse bioactivities such as anti-convulsant[1], anti-diarrheal[2], anti-ischemic[3], anti-platelet activating factor[4], antagonist[5], anti-histaminic[6], anti-microbial[7], anti-diabetic[8], cycloxygenase inhibitory[9], PAF Ca2+ channel blocker[10], cardio protective[11], anti-cancer[12], anti-HIV[13], non-peptide thrombin receptor antagonist[14] and tumor necrosis factor-α antagonist activities[15]. These observations led to the conception that CPTHZ would possess potential antimicrobial properties.

Biginelli reactions are well known for the synthesis of complex heterocyclic scaffolds having the rapeutic and pharmacological properties[16-18]. CPTHZ was synthesized by multi-component biginelli condensation of thiazolidine-2, 4-dione, urea and aromatic aldehydes[19]. To the best of our knowledge, neither the synthesis, nor the quantum chemical calculations of CPTHZ were illustrated yet.

2 Materials and Method

Progress of reaction was monitored by silica gel-G coated TLC plates in Ethyl acetate: Hexane system (7:3). The spot was visualized by exposing dry plate in iodine vapours. Melting point was determined by the melting point determination apparatus (TEMPO) in open capillary tubes and was uncorrected. Perkin–Elmer FTIR spectrophotometer and Bruker 300 MHz instrument (using $CDCl_3$ as a solvent and tetramethyl silane as an internal standard) were used for recording infrared (IR) and ^{1}H and ^{13}C NMR spectra respectively. Mass of the compound was also recorded by HRMS. Chemical shift value was expressed in delta parts per million (ppm). All chemicals were purchased from *Alfa Aesar* and *Sigma–Aldrich*. UV spectrum was recorded on UV–visible Double-Beam Spectrophotometer (systronic-2203) instrument (DMSO was used as a solvent).

2.1. General procedure for synthesis of (S)-7-(4-chlorophenyl)-6,7-dihydrothiazolo[4,5-d]pyrimidine-2,5(3H,4H)-dione (Scheme 1):

The compound CPTHZ was synthesized by known classical biginelli reaction[19]. 4-5 drops of conc. HCl added in the mixture of 0.01 mol of the thiazolidine-2,4-dione(1), 0.01 mol of 4-chlorobenzaldehyde (2), 0.015mol of urea(3) in 15 mL of ethanol and was refluxed for 8-10 h. The reaction was monitored on TLC and reaction mixture was left overnight. The solid thus formed was washed with luke warm water followed by washing with 10% ethanol and

*Corresponding author: (E-mail: abhabishnoi5@gmail.com, dr.abhabishnoi@gmail.com)

recrystallized with absolute ethanol. Yield: ~55%; m.p.: 225-230°C.

3 Computational methods

The various calculations were done using Density functional theory (DFT) method with B3LYP and CAM-B3LYP functions using 6-31G (d,p) basis atomic set. All the calculations and the analysis of results of CPTHZ were done with the help of gaussian 09 program package and gauss view 5.0 molecular visualization program[20-23]. All the vibrational frequencies and the optimized geometrical parameters were figured by applying hybrid functional B3LYP and CAM-B3LYP[24, 25] and basis set 6-31G(d,p) of DFT[26-28] and the donor–acceptor interactions were tallied by applying the second-order fock matrix[29]. Calculated UV–Vis spectrum was obtained by applying TD-DFT method. Density of electrons in various bonding and anti-bonding orbitals were shown by the Non Bonding Orbital properties.

4. Results and Discussion

4.1. Molecular geometry

Supplementary Table 1 shows different structural parameters of CPTHZ which were obtained by DFT technique. Any symmetry constraint was not visible during geometry optimization. Fig. 1a & 1b give the

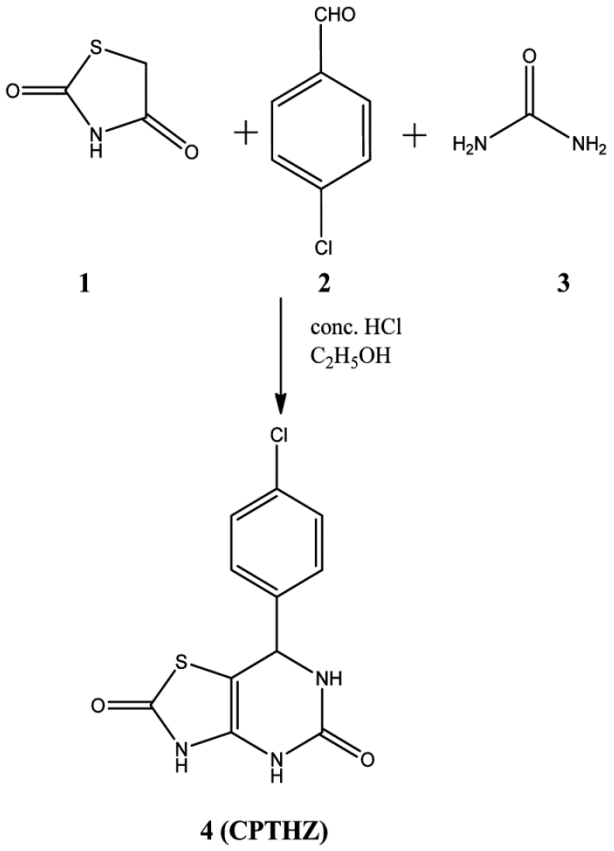

Scheme 1: Synthesis of CPTHZ

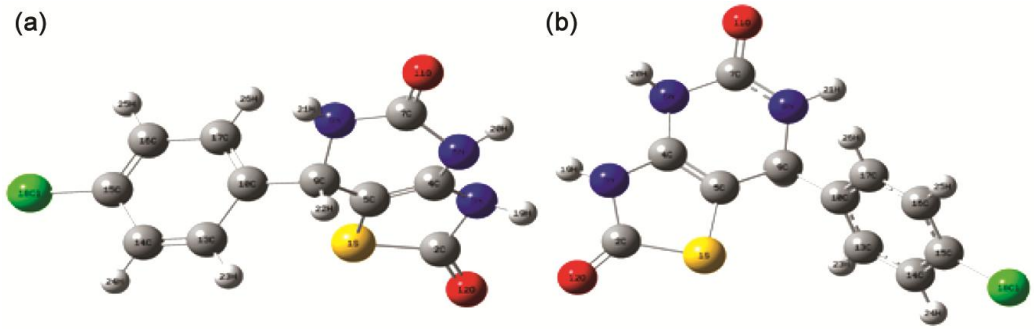

Fig. 1a & 1b — Optimized geometry of CPTHZ using B3LYP/6-31G(d,p) & CAM-B3LYP/6-31G(d,p) level of theory.

Table 1 — Experimental and calculated ^{1}H and ^{13}C NMR of CPTHZ

ATOM	B3LYP	CAM-B3LYP	Exp	ATOM	B3LYP	CAM-B3LYP	Exp
C2	167.41	168.34	168.14	H19	6.52	6.60	12.69
C4	123.07	123.45	129.86	H20	5.43	5.51	7.86
C5	92.96	89.15	124.79	H21	3.99	4.05	7.89
C7	143.86	144.88	167.72	H22	5.51	5.46	5.20
C9	63.5	58.40	129.86	H23	7.28	7.47	7.58-7.79
C10	140.75	140.15		H24	7.32	7.50	
C13	127.49	127.43	130-135.45	H25	7.51	7.67	
C14	126.54	126.35		H26	7.89	8.04	
C15	141.32	139.21					
C16	128.14	127.85					
C17	128.11	127.82					

information about the arrangements of different atoms in the molecule. The point group symmetry of the CPTHZ is C1.

4.2. ^{1}HNMR and ^{13}CNMR spectroscopy:

B3LYP/6-31G(d,p) and CAM- B3LYP/6-31G(d,p) basis set were used with GIAO approach for calculating ^{1}H and ^{13}C NMR chemical shifts[30,31]. The experimental and calculated values of ^{1}HNMR and ^{13}CNMR chemical shifts of CPTHZ were tabulated in Table 1. The experimental ^{1}H and ^{13}C NMR spectra of compound were given in supplementary Figs. S_1-S_2 respectively. Correlation between calculated and experimental ^{1}H NMR and ^{13}CNMR chemical shifts were shown in Fig. 2a & 2b.

4.3. UV–Visible absorption spectroscopy:

Solvent effect was detected by applying Integral Equation Formalism Polarizable Continuum Model (IEFPCM)[32]. The calculated and experimental UV-Vis spectra were shown in Fig. 3. The calculated UV data were ordered in Table 2 and compared with experimental UV data. Table 2 shows that HOMO to

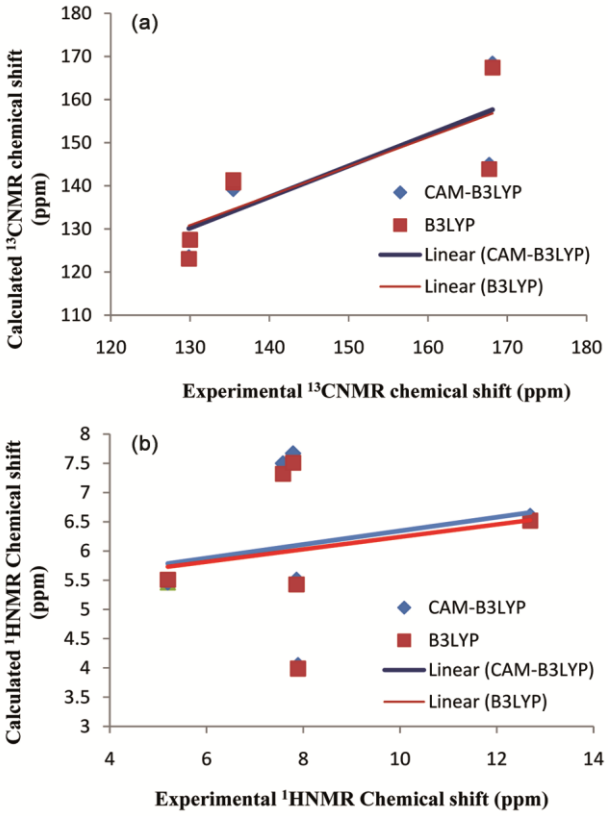

Fig. 2 — (a) Correlation graph between calculated and experimental ^{13}CNMR chemical shifts. (b) Correlation graph between calculated and experimental ^{1}H NMR chemical shifts.

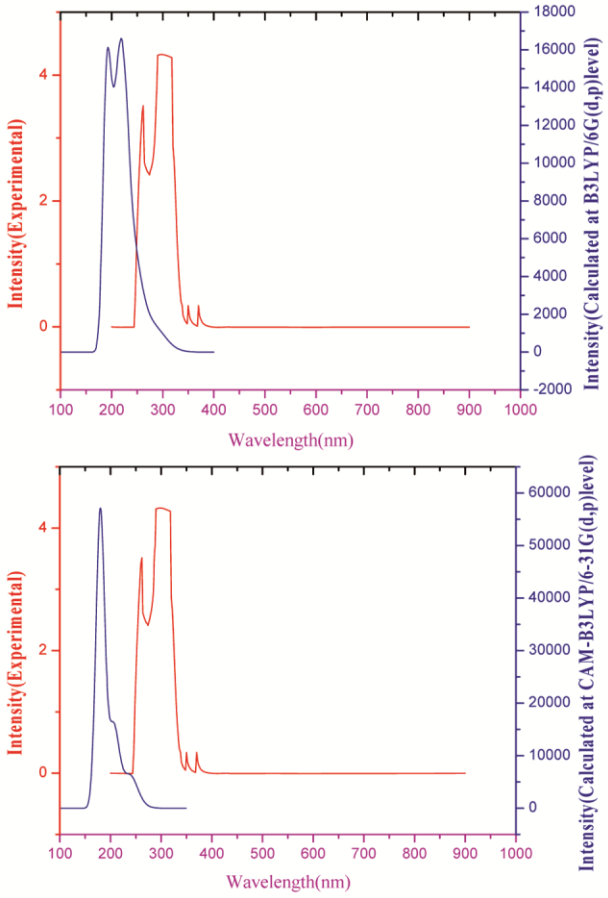

Fig. 3 — Experimental and calculated UV–visible spectra of the CPTHZ.

Table 2 — Experimental and theoretical absorption wavelength λ_{max} (nm), excitation energies E (eV) of CPTHZ

S. No	Electronic transitions (Molecular orbital involved)	Energy (in eV)	Calculated λ_{max}(in nm)	Absorbance	Oscillatory strength (*f*)	Percentage contribution of probable transition	Observed λ_{max}(in nm)
			B3LYP			B3LYP	
1	71→73 (H-1→L)	5.5780	222.27	0.385744	0.1773	37.53%	245
2	72→78 (H→L+5)	5.4662	226.82	3.513198	0.1189	46.47%	262
3	72→73(H→L)	4.1544	298.44	4.303171	0.0021	47.09%	310
			CAM-B3LYP			CAM-B3LYP	
4	72→75 (H→L+2)	5.1420	241.12		0.1330	17.99%	
5	71→73 (H-1→L)	5.9713	207.63	0.3857	0.2435	40.44%	245

LUMO transition [for B3LYP/6-31G(d,p)] and HOMO-1 to LUMO transition [for CAM-B3LYP/6-31G(d,p)] have highest percentage contribution and these transitions showed an intense electronic transition at 298.44nm and 207.63nm respectively, which were in good concord with the experimental data ($\lambda_{exp.}$ = 310 nm and 245 nm in DMSO respectively). In the CPTHZ most of the transitions appeared due to σ→σ* transitions. Molecular orbitals of the compound and their electronic transitions were shown in Fig. 4a & 4b. HOMO was mainly localized on the pyrimidine ring and thiazolidinone ring. LUMO was delocalized over the aromatic ring, nitrogen atom nearest to the aromatic ring and carbonyl function (C=O) of pyrimidine ring. The value of the energy gap between HOMO and LUMO was 4.1544eV [obtained by B3LYP] and energy gap between HOMO-1 and LUMO is 5.9713 eV [CAM-B3LYP].

4.4. Vibrational assignments:

All types of vibrations possess by the compound CPTHZ and their corresponding wave numbers were given in Table 3. There was a good agreement between experimental and calculated wave numbers as shown by the value of correlation coefficient R^2 =0.995 and 0.989 obtained by using B3LYP and CAM-B3LYP respectively Fig. 5. The IR spectra obtained experimentally and theoretically [using B3LYP and CAM-B3LYP/6-31G(d,p)] were shown in Fig. 6.

4.5. Mulliken charge distribution:

Mulliken charges obtained through two different sets were given in table 4 and plot obtained was given in Fig. 7. From the Fig. 7 it was evident that negative charges were delocalized over N3, C5, N6, O11, O12 and C15 at the same time it was found that more positive charges were delocalized over S1, C2, C4, C7, C9 and C10. C2 and C7 carried more positive charges as they were directly bounded to oxygen atom.

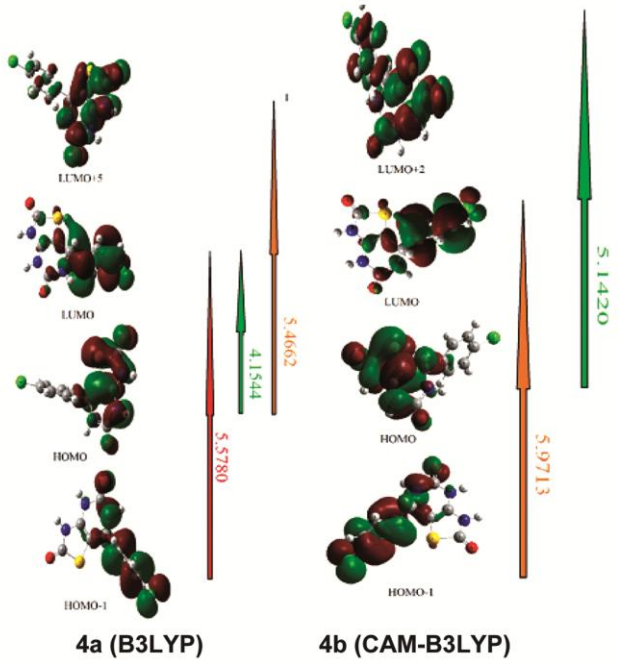

Fig. 4a & 4b — Electronic transitions.

Table 3 — Experimental and calculated vibrational frequencies in cm^{-1}

Experimental	Calculated (B3LYP) (cm^{-1})	Calculated (CAM-B3LYP) (cm^{-1})	Vibrational Assignment	Characteristic Absorptions (cm^{-1})
3340-3360	3641.81 3655.72	3660	Asymmetric N-H stretching	The N-H stretching vibrations are obtained between 3500-3140cm^{-1}.
3145.90	3181.98	3201.61	Aromatic = C-H stretching	The aromatic C-H stretching vibrations are normally found between 3100 and 3000 cm^{-1} due to aromatic C-H stretching vibrations. In the compound CPTHZ the aromatic ring is attached to another 6 member ring which in turn further fussed with a 5 member ring therefore aromatic C-H stretching vibrations appeared at lower frequency
3049.96	2957.57	2985.39	Aliphatic -C-H stretching	Aliphatic -C-H stretching vibrations are obtained between 2850-3000cm^{-1}.
1722.43 1755.22	1825.64 1838.80	1830.82 1842.26	C=O stretching	Amide shows lower carbonyl stretching frequency, absorbing around 1650-1690 cm^{-1}. In conjugated amides the carbonyl stretching frequency is lowered.
1608.63	1729.57	1744.82	C=C stretching	C=C stretching vibrations are obtained between1550-1640cm^{-1}.
1585.49	1544.32	1562.11	N-H in plane bending	The N-H bending vibrations are obtained between1550-1640cm^{-1}.
1010.70-1296.16	1079.63-1295.12	1092.57-1318.34	C-N stretching	The C-N stretching vibrations are obtained between 1030- 1230cm^{-1}.
740	744.31	707.11	C-Cl stretching	The C-Cl stretching vibrations are obtained between 850-550cm^{-1}.
698.23	698.75	675.32	C-S stretching	C-S stretchings occur near 700-600cm^{-1}.

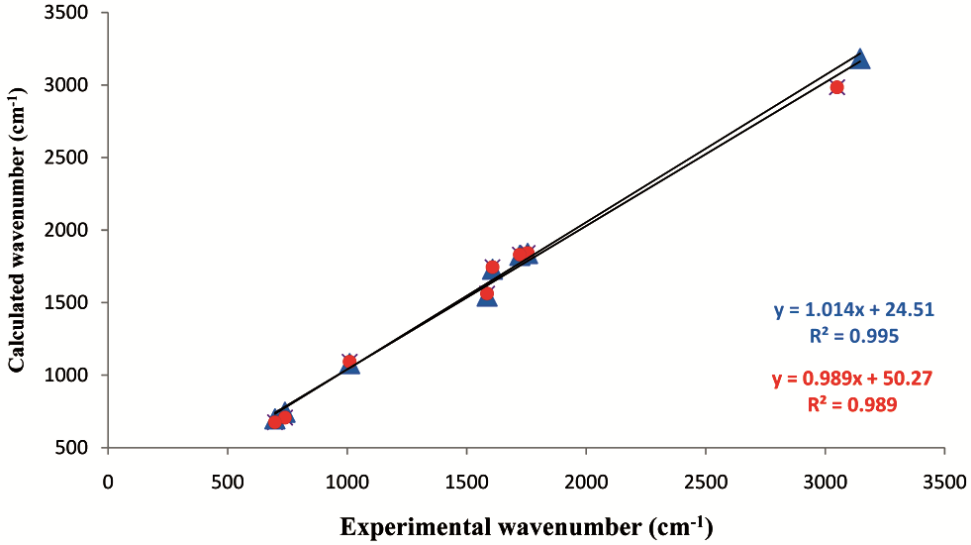

Fig. 5 — Correlation graph between calculated (B3LYP and CAM-B3LYP) and experimental wave numbers of CPTHZ.

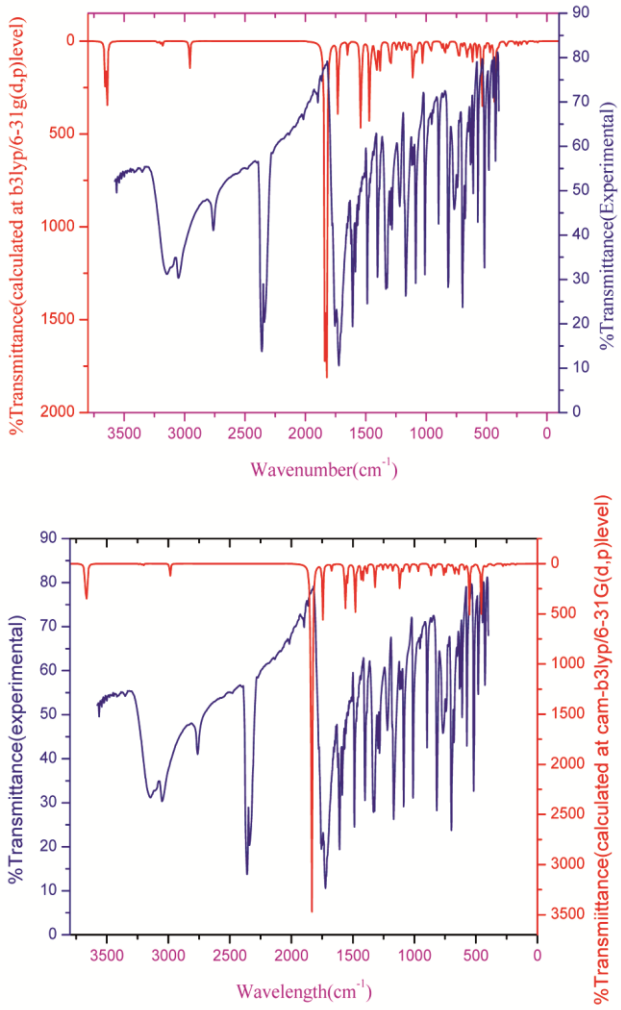

Fig. 6 — Experimental and theoretical IR spectra of CPTHZ.

Table 4 — The Mulliken charge distribution calculated at B3LYP and CAM-B3LYP/6-31G(d,p) level

Atoms	Atomic Charges B3LYP	Atomic Charges CAM-B3LYP
1 S	0.217386	0.209222
2 C	0.411126	0.422044
3 N	-0.33796	-0.303644
4 C	0.609682	0.590721
5 C	-0.22423	-0.242126
6 N	-0.37044	-0.367685
7 C	0.69828	0.731654
8 N	-0.29657	-0.298068
9 C	0.150643	0.169885
10 C	0.042535	0.088877
11 O	-0.43961	-0.509937
12 O	-0.45315	-0.469315
13 C	-0.00699	-0.02497
14 C	0.03172	0.050148
15 C	-0.08901	-0.096323
16 C	0.032227	0.050193
17 C	0.025399	0.014907
18 C	-0.00103	-0.015585

4.6. Molecular electrostatic potential:

Gauss view software was used for plotting the MESP map of the CPTHZ shown in Fig. 8. The different colors in MESP map give information about electron rich and electron poor regions, which are referred by the red and blue regions respectively while the neutral regions are shown by green color. Both the MESP plot obtained by using B3LYP and CAM-B3LYP levels showed that the H atoms attached to N atoms and region around N atoms bear the maximum brunt of positive potential, consequently it was expected that nucleophilic attack might occurs at this site[33-35].

4.7. Natural bond orbital analysis:

The second-order Fock matrix described the donor–acceptor interactions in NBO analysis. A useful tool implemented to perform the Natural Bond Orbital (NBO) calculations was Gaussian09 package at the B3LYP/6-31G(d,p) and CAM-B3LYP/6-31G(d,p) methods[36]. In the Table 5a and 5b all the effective intramolecular and intermolecular charge transfers and occupancy of electrons were tabulated.

4.8. Non linear optical (NLO) analysis:

NLO effect has great importance in the current research[37-39]. In NLO study the effect of applied electromagnetic fields on compound to generate new electromagnetic fields is taken into consideration. The B3LYP/6-31G(d,p) basis set and CAM- B3LYP/6-31G(d,p) basis set based on the finite field approach were used to calculate first hyperpolarizability of the CPTHZ. First static hyperpolarizability obtained, indicated that title molecule could be used as an

Table 5a — Second order perturbation theory analysis of Fock matrix in NBO basis of the title compound using B3LYP

Donor	Type	Occupancy (ED/e)	Acceptor	Type	Occupancy (ED/e)	E(2)*	Ej-Ei**	Fij***	Charge transfer
BD(1)N8-H21	σ	1.9816	BD*(1)N6-C7	σ *	0.08397	5.31	1.06	0.068	σ (N8-H21)→ σ *(N6-C7)
BD(2)C10-C13	σ	1.6714	BD*(2)C14-C15	σ *	0.37608	20.64	0.27	0.068	σ (C10-C13)→ σ *(C14-C15)
BD(2)C10-C13	σ	1.6714	BD*(2)C16-C17	σ *	0.30143	19.82	0.29	0.068	σ (C10-C13)→ σ *(C16-C17)
BD*(2)C14-C15	σ	1.6808	BD*(2)C10-C13	σ *	0.34894	18.77	0.30	0.067	σ (C14-C15)→ σ *(C10-C13)
BD*(2)C14-C15	σ	1.6808	BD*(2)C16-C17	σ *	0.30143	18.62	0.30	0.067	σ (C14-C15)→ σ *(C16-C17)
BD(2)C16-C17	σ	1.6690	BD*(2)C10-C13	σ *	0.34894	19.74	0.28	0.067	σ (C16-C17)→ σ *(C10-C13)
BD(2)C16-C17	σ	1.6690	BD*(2)C14-C15	σ *	0.37604	20.81	0.27	0.068	σ (C16-C17)→ σ *(C14-C15)
LP(2)S1	n	1.7555	BD*(2)C2-O12	π*	0.38559	27.68	0.24	0.076	n (S1)→ π*(C2-O12)
LP(2)S1	n	1.7555	BD*(2)C4-C5	π*	0.33303	16.57	0.27	0.061	n (S1)→ π*(C4-C5)
LP(1)N3	n	1.672	BD*(2)C2-O12	π*	0.38559	55.08	0.28	0112	n(N3)→ π*(C2-O12)
LP(1)N3	π	1.672	BD*(2)C4-C5	n	0.33303	40.73	0.30	0.099	π(N3)→n(C4-C5)
LP(1)N6	n	1.731	BD*(2)C4-C5	π*	0.33303	40.60	0.30	0.100	n(N6)→π*(C4-C5)
LP(1)N8	n	1.7426	BD*(1)C9-H22	σ *	0.03739	5.92	0.69	0.060	n(N8)→ σ *(C9-H22)
LP(2)O11	σ	1.8397	BD*(1)N6-C7	n	0.08397	27.40	0.65	0.121	σ(O11)→n(N6-C7)
LP(2)O11	σ	1.8397	BD*(1)C7-N8	n	0.07545	25.44	0.69	0.121	σ(O11) →n(C7-N8)
LP(2)O12	n	1.7956	BD*(1)S1-C2	σ *	0.13057	36.06	0.40	0.109	n(O12)→ σ *(S1-C2)
LP(2)O12	σ	1.7956	BD*(1)C2-N3	n	0.08926	26.49	0.66	0.121	σ(O12)→n(C2-N3)
LP(1)N6	n	1.731	BD*(2)C7-O11	π*	0.36408	45.00	0.31	0.107	n(N6)→ π*(C7-O11)
LP(1)N8	n	1.7426	BD*(2)C7-O11	π*	0.36408	59.11	0.28	0.118	n (N8)→π*(C7-O11)

Table 5b — Second order perturbation theory analysis of Fock matrix in NBO basis of the title compound using CAM-B3LYP

Donor	Type	Occupancy (ED/e)	Acceptor	Type	Occupancy (ED/e)	E(2)*	Ej-Ei**	Fij***	Charge transfer
BD(1)S1-C5	σ	1.96973	BD*(1)C4-N6	σ *	0.03140	8.06	1.21	0.088	σ (S1-C5) → σ *(C4-N6)
BD(2)C10-C13	σ	1.67380	BD*(2)C14-C15	σ *	0.37089	30.29	0.35	0.093	σ(C10-C13) → σ *(C14-C15)
BD(2)C10-C13	σ	1.67380	BD*(2)C16-C17	π*	0.30097	29.0	0.37	0.093	σ (C10-C13) → π*(C16-C17)
BD(1)C13-C14	π	1.97225	BD*(1)C15-Cl18	σ *	0.02710	5.23	0.98	0.064	π(C13-C14) → σ *(C15-Cl18)
BD(2)C14-C15	σ	1.68181	BD*(2)C10-C13	σ *	0.34555	28.52	0.38	0.094	σ(C14-C15) → σ *(C10-C13)
BD(2)C14-C15	σ	1.68181	BD*(2)C16-C17	π*	0.30097	27.48	0.38	0.092	σ(C14-C15) → π*(C16-C17)
BD(1)C16-C17	σ	1.97263	BD*(1)C15-Cl18	σ *	0.02710	5.09	0.98	0.063	σ(C16-C17) → σ *(C15-Cl18)
BD(2)C16-C17	σ	1.66775	BD*(2)C10-C13	σ *	0.34555	29.45	0.36	0.093	σ(C16-C17) → σ *(C10-C13)
BD(2)C16-C17	σ	1.66775	BD*(2)C14-C15	σ *	0.37089	30.91	0.35	0.094	σ(C16-C17) → σ *(C14-C15)
LP(2)S1	n	1.77410	BD*(2)C2-O12	π*	0.36136	36.40	0.33	0.101	n(S1) → π*(C2-O12)
LP(2)S1	n	1.77410	BD*(2)C4-C5	π*	0.31285	20.51	0.36	0.078	n(S1) → π*(C4- C5)
LP(1)N3	n	1.68560	BD*(2)C2-O12	π*	0.36136	69.85	0.37	0.144	n(N3) → π*(C2-O12)
LP(1)N3	n	1.68560	BD*(2)C4-C5	π*	0.31285	49.16	0.39	0.124	n(N3) → π*(C4-C5)
LP(1)N6	n	1.74460	BD*(2)C7-O11	π*	0.32549	46.58	0.44	0.130	n(N6) → π*(C7-O11)
LP(1)N8	n	1.75422	BD*(2)C7-O11	π*	0.32549	62.74	0.41	0.147	n(N8) → π*(C7-O11)
LP(1)N8	n	1.75422	BD*(1)C9-H22	σ *	0.03447	6.83	0.80	0.070	n(N8) → σ *(C9-H22)
LP(2)O11	σ	1.84715	BD*(1)N6-C7	n	0.08095	32.08	0.77	0.143	σ(O11) → n(N6-C7)
LP(2)O11	σ	1.84715	BD*(1)C7-N8	n	0.07278	29.55	0.82	0.141	σ(O11) → n(C7-N8)
LP(2)O12	n	1.80755	BD*(1)S1-C2	σ *	0.11973	41.67	0.51	0.132	n(O12) → σ *(S1-C2)
LP(2)O12	σ	1.80755	BD*(1)C2-N3	n	0.08728	31.71	0.77	0.144	σ(O12) → n(C2-N3)
LP(3)Cl18	n	1.93657	BD*(2)C14-C15	σ *	0.37089	14.57	0.43	0.076	n(Cl18) → σ *(C14-C15)

attractive future NLO material. Electrophilic and nucleophilic regions were given in MESP plot. The first hyperpolarizability was described by 3x3x3 matrix. The 27 components of the matrix reduced to 10 components due to Kleinman symmetry[40].The magnitude of total dipole moment μ_{tot}, the average polarizability α_{tot} and the first hyperpolarizability β_{tot} were calculated by the Eq. 1-3 and listed in Table 6.

$$\mu_{tot} = \left(\mu_x^2 + \mu_y^2 + \mu_z^2\right)^{1/2} \quad \ldots (1)$$

$$\alpha_{tot} = \frac{1}{3}\left(\alpha_{xx} + \alpha_{yy} + \alpha_{zz}\right) \quad \ldots (2)$$

$$\langle\beta\rangle = \left[\begin{array}{l}\left(\beta_{xxx} + \beta_{xyy} + \beta_{xzz}\right)^2 + \left(\beta_{yyy} + \beta_{yzz} + \beta_{yxx}\right)^2 \\ + \left(\beta_{zzz} + \beta_{zxx} + \beta_{zyy}\right)^2\end{array}\right]^{1/2} \quad \ldots (3)$$

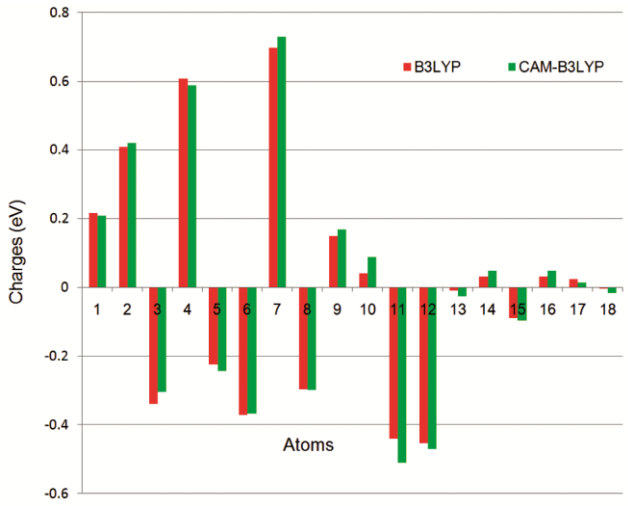

Fig. 7 — Mulliken charge distribution in CPTHZ.

The calculated dipole moment obtained by using B3LYP/6-31G(d,p) and CAM- B3LYP/6-31G(d,p) basis sets were equal to 2.0378D and 1.7296D respectively. The calculated polarizability α_{tot} was equal to 23.9335×10^{-24}esu for B3LYP level and 3.4195×10^{-24}esu for CAM-B3LYP level. The calculated first hyperpolarizability of the CPTHZ was 222.18×10^{-30} esu for B3LYP level and $0.0003954 \times 10^{-30}$esu for CAM- B3LYP level. Out of these values, value obtained through B3LYP was greater than that of the standard NLO material urea (0.13×10^{-30} esu).[41]

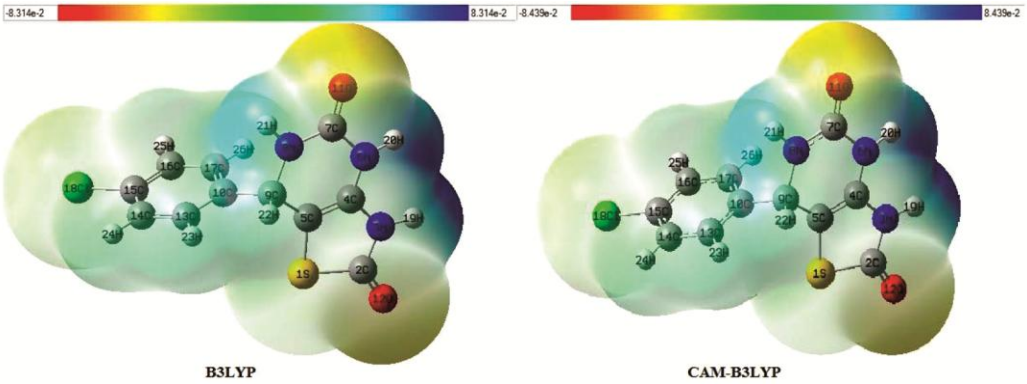

Fig. 8 — The molecular electrostatic potential of CPTHZ.

Table 6 — Dipole moment μ_{tot}, polarizability α_{tot} and first order hyperpolarizability β_{tot} data for CPTHZ

	Dipole Moment			Static Hyperpolarizability (in esu)	
	B3LYP	CAM-B3LYP		B3LYP	CAM-B3LYP
μ_x	0.5982	0.6951	β_{xxx}	171.688	0.634762
μ_y	1.7691	1.4641	β_{xxy}	67.5563	-0.73349
μ_z	0.8155	0.6038	β_{xyy}	-88.6667	-0.61578
μ_{tot}	2.0378	1.7296	β_{yyy}	-65.5031	0.360506
	Polarizability (in esu)		β_{xxz}	60.3955	-0.09595
α_{xx}	218.854	30.93497	β_{xyz}	-11.6208	0.379305
α_{xy}	12.9545	1.980115	β_{yyz}	43.4635	-0.07451
α_{yy}	145.31	20.82403	β_{xzz}	-11.3893	0.046685
α_{xz}	-13.589	-1.87955	β_{yzz}	8.54291	0.471237
α_{yz}	-6.3719	-1.02335	β_{zzz}	56.157	0.360506
α_{zz}	120.32	17.46167	β_{tot}	222.18×10^{-30}	$0.0003954 \times 10^{-30}$
α_{tot}	23.9335×10^{-24}	3.4195×10^{-24}			

4.9. Thermodynamic properties:

All the thermodynamic parameters were recorded by DFT using B3LYP and CAM-B3LYP functional with 6-31G(d,p) basis set. The values of some thermodynamic parameters of CPTHZ were shown in the table 7.

All these parameters were obtained at standard temperature 298.15K. The standard statistical thermodynamic functions were recorded at temperatures 100–500K for CPTHZ on the basis of vibrational analysis and listed in table 8.

It was evident from the table 8 that the standard statistical thermodynamic functions such as heat capacity and entropy increase with temperature ranging from 100 K to 500 K[42,43]. Correlation graphs for heat capacity and entropy calculated at different temperatures were shown in Fig. 9.

4.10. Chemical reactivity descriptor:

4.10.1. Global reactivity descriptors:

Global reactivity descriptors were taken into consideration for predicting the reactivity of the molecule. All the Global reactivity descriptors of

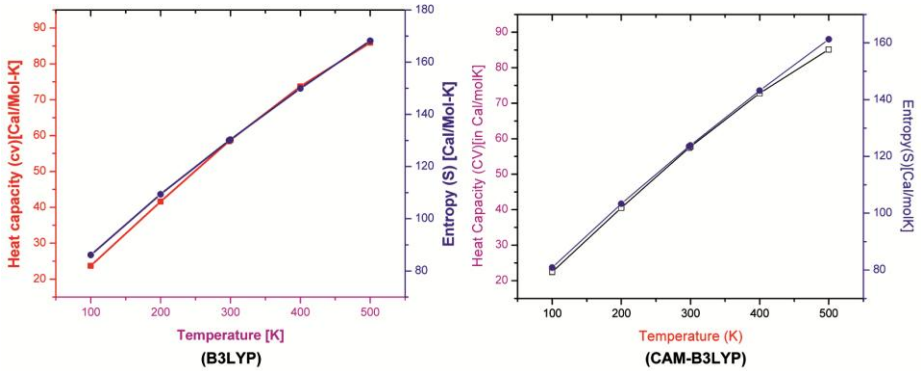

Fig. 9 — Correlation graphs of heat capacity and entropy calculated at different temperatures.

Table 7 — Calculated thermodynamic parameters of CPTHZ at standard temperature 298.15 K

Parameters	B3LYP6-31G(d,p)	CAM-B3LYP6-31G(d,p)
Zero point vibrational energy (Kcal/mol)	479741.6 (Joules/Mol)	485808.2 (Joules/Mol)
	114.66099 (Kcal/Mol)	116.11094 (Kcal/Mol)
Rotational temperature(K)	0.02635	0.02635
	0.00948	0.00948
	0.00762	0.00762
Rotational constant(GHZ)		
X	0.54908	0.02635
Y	0.19753	0.00948
Z	0.15883	0.00762
Total energy E_{total}(Kcal/mol)	124.368	125.434
Translational	0.889	0.54904
Rotational	0.889	0.19753
Vibrational	122.590	0.15883
	B3LYP (Hartree/particle)	CAM-B3LYP (Hartree/particle)
Sum of electronic and zero-point Energies	-1596.935922	-1596.577614
Sum of electronic and thermal Energies	-1596.920453	-1596.562758
Sum of electronic and thermal Enthalpies	-1596.919509	-1596.561813
Sum of electronic and thermal Free Energies	-1596.981268	-1596.620498

Table 8 — Thermodynamic functions at different temperatures

Temperature [K]	Heat capacity(CV) [Cal/molK](B3LYP)	Entropy(S) [Cal/molK](B3LYP)	Heat capacity(CV) [Cal/molK](CAM-B3LYP)	Entropy(S) [Cal/molK](CAM-B3LYP)
100	23.688	86.123	22.464	80.864
200	41.606	109.383	40.516	103.33
298	58.454	129.983	57.443	123.511
300	58.754	130.358	57.745	123.88
400	73.695	149.941	72.804	143.188
500	85.907	168.191	85.139	161.253

CPTHZ were calculated and texted in the table 9. A global reactivity index is a positive and definite quantity and, an electrophilicity index (ω). Electrophilic charge transfer (ECT)[44] can be obtained by calculating the difference between the ΔN_{max} values of interacting molecules. The lower value of electrophilicity index ω =-0.0348eV for B3LYP and ω =0.04944eV for CAM-B3LYP of CPTHZ indicatds that it was a weak electrophile.

4.10.2. Local reactivity descriptors:

Fukui function (f_K) gives various information about the molecule. Fukui functions ($f_\kappa^{\pm}$), local softness ($S_\kappa^{\pm}$) and local electrophilicity indices ($\omega_K^{\pm}$)[45,46] for selected atomic sites of molecule were listed in table 10.

Table 9 — Calculated frontier molecular orbitals (ƐLUMO, ƐHOMO), band gap (ƐLUMO-ƐHOMO), ionization potential (IP), electron affinity (EA), electronegativity (χ), global hardness(η), chemical potential (μ), global electrophilicity index (ω), global softness (S) and additional electronic charge (ΔN_{max}) of CPTHZ

	ε_H	ε_L	$\varepsilon_H - \varepsilon_L$	IP	EA	
B3LYP	-0.2038	-0.0253	-0.1785	0.2038	0.0253	
CAM-B3LYP	-0.2564	0.02185	-0.2783	0.2564	-0.0218	
	χ	η	μ	Ω	S	ΔN_{max}
B3LYP	0.1145	-0.1145	0.0892	-0.0348	-0.0573	0.7793
CAM-B3LYP	0.1173	0.13916	-0.1173	0.04944	3.5929	0.8429

Table 10 — Hirshfeld population analysis: Fukui functions (fk^+, fk^-), Local softnesses (sk^+, sk^-) in eV, local electrophilicity indices (ωk^+, ωk^-) in eV for selected atomic sites of CPTHZ

Atom(B3LYP /CAM-B3LYP)	qN	qN+1	qN-1	fk+	fk-	sk+	sk-	ωk+	ωk-
S_1	0.2174	0.4324	0.1220	0.2150	0.0953	0.0554	0.0246	0.7872	0.3490
	0.2092	0.4465	0.1220	0.2373	0.0871	0.0612	0.0225	0.8688	0.3191
C_2	0.4111	0.4322	0.3909	0.0211	0.0201	0.0054	0.0052	0.0774	0.0738
	0.4220	0.4321	0.3909	0.0101	0.0310	0.0026	0.008	0.0371	0.1137
N_3	0.3379	-0.2294	-0.3420	0.1084	0.0040	0.0280	0.0010	0.3971	0.0148
	0.3036	-0.2258	-0.3420	0.0778	0.0384	0.0201	0.0099	0.2849	0.1404
C_4	0.6096	0.6631	0.5463	0.0534	0.0633	0.0138	0.0163	0.1957	0.2317
	0.5907	0.6644	0.5463	0.0737	0.0443	0.0190	0.0114	0.2699	0.1623
C_5	0.2242	-0.1811	-0.2368	0.0430	0.0126	0.0111	0.0033	0.1576	0.0463
	0.2421	-0.1714	-0.2368	0.0706	-0.0052	0.0182	-0.0013	0.2586	-0.019
N_6	0.3704	-0.2731	-0.4049	0.0973	0.0345	0.0251	0.0089	0.3562	0.1263
	0.3676	-0.2617	-0.4049	0.1059	0.0372	0.0273	0.0096	0.3879	0.1364
C_7	0.6982	0.7627	0.7002	0.0644	-0.0019	0.0166	-0.0005	0.2360	-0.007
	0.7316	0.7512	0.7002	0.0196	0.0314	0.0050	0.0080	0.0719	0.1150
N_8	0.2965	-0.2526	-0.3098	0.0439	0.0132	0.0113	0.0034	0.1609	0.0485
	0.2980	-0.2495	-0.3098	0.0485	0.0117	0.0125	0.0030	0.1777	0.0429
C_9	0.1506	0.1950	0.1191	0.0444	0.0314	0.0115	0.0081	0.1627	0.1151
	0.1698	0.2037	0.1191	0.0338	0.0506	0.0087	0.0130	0.1237	0.1855
C_{10}	0.0425	0.0946	0.1286	0.0521	-0.0860	0.0134	-0.0222	0.1908	-0.315
	0.0888	0.0795	0.1286	-0.009	-0.0397	-0.0024	-0.0102	-0.034	-0.145
O_{11}	0.4396	-0.4414	-0.5723	0.0018	0.1326	-0.0005	0.0342	-0.007	0.4858
	0.5099	-0.4361	-0.5723	0.0737	0.0623	0.0190	0.0160	0.2701	0.2283
O_{12}	0.4531	-0.3614	-0.5319	0.0917	0.0788	0.0236	0.0203	0.3357	0.2885
	0.4693	-0.3528	-0.5319	0.1164	0.0626	0.0300	0.0161	0.4263	0.2293
C_{13}	0.0069	-0.0041	-0.1566	0.0028	0.1496	0.0007	0.0386	0.0103	0.5479
	0.0249	-0.0068	-0.1566	0.0181	0.1316	0.0046	0.0339	0.0664	0.4821
C_{14}	0.0317	0.0941	-0.0755	0.0624	0.1072	0.0161	0.0276	0.2286	0.3927
	0.0501	0.0894	-0.0755	0.0393	0.1257	0.0101	0.0323	0.1438	0.4601
C_{15}	0.0890	-0.0924	-0.0823	-0.003	-0.0066	-0.0009	-0.0017	-0.013	-0.024
	0.0963	-0.0947	-0.0823	0.0016	-0.0139	0.0004	-0.0036	0.0058	-0.051
C_{16}	0.0322	0.0885	-0.0809	0.0563	0.1131	0.0145	0.0291	0.2061	0.4142
	0.0501	0.0864	-0.0809	0.0362	0.1311	0.0093	0.0337	0.1325	0.4800
C_{17}	0.0253	0.0063	-0.0937	-0.019	0.1191	-0.0049	0.0307	-0.070	0.4361
	0.0149	0.0063	-0.0937	-0.009	0.1086	-0.0022	0.0280	-0.031	0.3977
Cl_{18}	0.0010	0.0665	-0.1202	0.0675	0.1191	0.0174	0.0307	0.2472	0.4362
	0.0155	0.0455	-0.1202	0.0611	0.1046	0.0157	0.0269	0.2237	0.3830

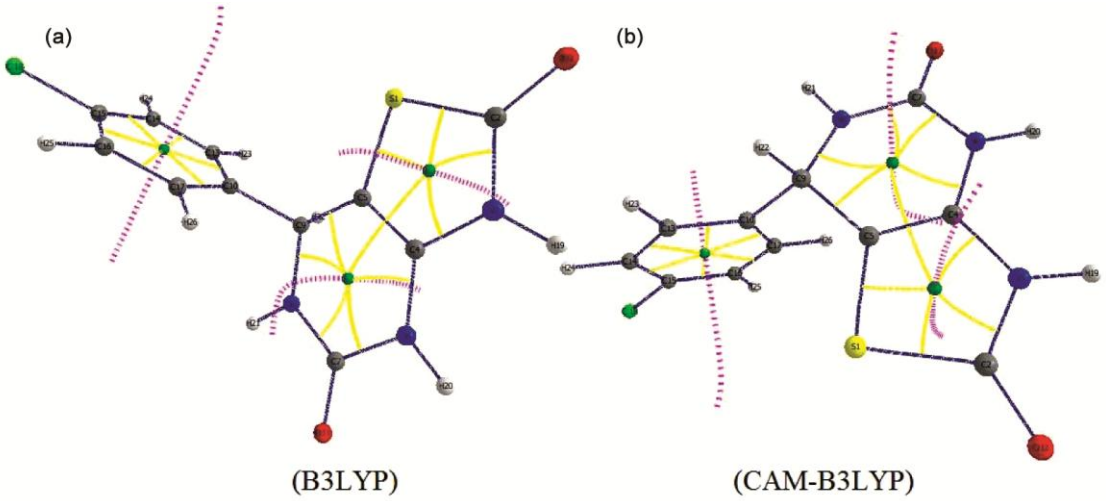

Fig. 10a & 10b — Molecular graph of the compound CPTHZ using AIM program at B3LYP and CAM-B3LYP/6- 31G(d,p) level ring critical points (small green sphere), bond critical paths (blue lines), ring critical point to bond critical paths (yellow lines) and ring critical point attractor path (purple lines).

From Table 10 it can be observed that N3, N6, O12 and S1 sites were more prone to nucleophilic attack because of the relative high value of local reactivity descriptors (S_κ^+, f_κ^+, ω_K^+) whereas C13, O11, C16 and C14 sites were more prone to electrophilic attack because of the relative high value of local reactivity descriptors (S_κ^-, f_κ^-, ω_K^-).

4.11. AIM Analysis:

AIM studies give information about hydrogen bonding and alignment of atoms in molecule. AIM data obtained by using B3LYP and CAM-B3LYP clearly indicated that no intermolecular hydrogen bonding was found in CPTHZ and molecular graphs for compound were given in Fig. 10a & 10b.

Conclusion:

(S)-7-(4-chlorophenyl)-6,7-dihydrothiazolo[4,5-d]pyrimidine-2,5(3H,4H)-dione CPTHZ was synthesized and identified by ^{1}H , ^{13}C NMR, UV–visible and FTIR. The value of the energy gap between HOMO and LUMO is 4.1544eV [obtained by B3LYP] and energy gap between HOMO-1 and LUMO is 5.9713 eV [CAM-B3LYP]. Most of the electronic transitions are (σ→σ*) transitions. NBO results reflect the charge transfer within the molecule. The first hyper polarizability of the CPTHZ obtained through B3LYP and CAM-B3LYP are 222.18×10^{-30} and $0.0003954 \times 10^{-30}$ respectively. These values enable CPTHZ to be a potential candidate for nonlinear optical applications. The values of electrophilicity index ω of product CPTHZ calculated through B3LYP and CAM-B3LYP are -0.0348 and 0.04944 indicate that it is a weak electrophile. The value of local reactivity descriptors (S_κ^-, f_κ^-, ω_K^-) show that N3, N6, O12 and S1 sites are more prone to nucleophilic attack because of the relative high value of local reactivity descriptors (S_κ^+, f_κ^+, ω_K^+) whereas C13, O11, C16 and C14 sites are more prone to electrophilic attack. The thermo dynamical parameters like heat capacity and entropy were found to increase with the increase of the temperature.

Acknowledgements:

The authors are thankful to the Head, Department of Chemistry, Lucknow University, Lucknow, for providing laboratory facilities and UV, FTIR, NMR facilities.

References:

1 Ergene N & Capan G, *Il Farmaco*, 49 (1994) 449.
2 Diurno M V, Mazzoni O, Izzo A A & Bolognese A, *Il Farmaco*, 52 (1997) 2375.
3 Adachi Y, Suzuki Y, Homma N, Fukazawa M, Tamura K, Nishie I & Kuromaru O, *Eur J Pharmacol*, 367 (1999) 267.
4 Tanabe Y, Yamamoto H, Murakami M, Yanagi K, Kubota Y, Okumura H, Sanemitsu Y & Suzukamo G, *J Chem Soc Perkin Trans*, 7 (1995) 935.
5 Tanabe Y, Suzukamo G, Komuro Y, Imanishi N, Morooka S, Enomoto M, Kojima A, Sanemitsu Y & Mizutani M, *Tetrahedron Lett*, 32 (1991) 379.
6 Diurno M V, Mazzoni O, Correale G & Monterry I G, *Il Farmaco*, 54 (1999) 579.
7 Sharma R C & Kumar D, *J Indian Chem Soc*, 77 (2000) 492.
8 Ueno H, Oe T, Snehiro I & Nakamura S, *US Patent*, 5594116 (1997).

9 Ottaná R, Mazzon E, Dugo L, Monforte F, Maccari R, Sautebin L, De Luca G, Vigorita M G, Alcaro S & Ortuso F, *Eur J Pharmacol*, 448 (2002) 71.
10 Kato T, Ozaki T & Tamura K, *J Med Chem*, 42 (1999) 3134.
11 Kato T, Ozaki T & Ohi N, *Tetrahedron: Asymmetry*, (1999) 103963.
12 Ebeid M Y, Fathallah O A, El-Zaher M I, Kamel M M, Abdon W A & Anwar M M, *Bull Fac Pharm*, 34 (1996) 125.
13 Rawal R K, Prabhakar Y S, Katti S B & De Clercq E, *Bioorg Med Chem*, 13 (2005) 6771.
14 Kato Y, Kita Y, Nishio M, Hirasawa Y, Ito K, Yamanaka T, Motoyama Y & Seki J, *Eur J Pharmacol*, 384 (1999) 197.
15 Voss M E, Carter P H, Tebben A J, Scherle P A, Brown G D, Thompson L A, Xu M, Lo Y C & Yang L R R Q, *Bioorg Med Chem Lett*, 13 (2003) 533.
16 Kappe C O, *Tetrahedron*, 49 (1993) 6937.
17 Rovnyak G C, Kimball S D, Beyer B, Cucinotta G, Dimarco J D, Gougoutas J, Hedberg A, Malley M, Mccarthy J P, Zhang R & Moreland S, *J Med Chem*, 38 (1995) 119.
18 Atwal K S, Rovnyak G C, Kimball S D, Floyd D M, Moreland S, Swanson B N, Gougoutas J Z, Schwartz J, Smillie K M & Malley M F, *J Med Chem*, 33 (1990) 2629.
19 Zhu Y, Huang S & Pan Y, *Eur J Org Chem*, (2005) 2354.
20 Frisch M J, *et.al.*, Gaussian 03, Revision C.02, Gaussian Inc, Wallingford, CT, (2004).
21 Frisch M J, *et.al.*, Gaussian 09, Revision A.1, Gaussian Inc, Wallingford, CT, (2009).
22 Pittsburgh P A, Computer program Gauss View 3.09, Ver 2, Gaussian Inc, (SD-008).
23 Frisch E, Hratchian H P, Dennington I R D, Keith T A, Millam J, Nielsen A B, Holder A J & Hiscocks J, Gaussian Inc, GaussView Version 5.0.8, (2009).
24 Becke A D, *J Chem Phys*, 98 (1993) 5648.
25 Lee C T, Yang W T & Parr R G B, *Phys Rev*, 37 (1988) 785.
26 Karabacak M, *J Mol Struct*, 919 (2009) 215.
27 Petersson D A & Allaham M A, *J Chem Phys*, 94 (1991) 6081.
28 Petersson G A, Bennett A, Tensfeldt T G, Allaham M A & Mantzaris W A J, *J Chem Phys*, 89 (1988) 2193.
29 Sarafran M, Komasa A & Adamska E B, *J Mol Struct*, 82 (2007) 7101.
30 Wolinski K, Hinton J F & Pulay P, *J Am Chem Soc*, 112 (1990) 8251.
31 Zhengyu Z, Aiping F & Dongmei D, *J Quantum Chem*, 78 (2000) 186.
32 El-Shwiniy W H & Zordoc W A, *Spetrochim Acta A*, 199 (2018) 290.
33 Joshi B D, Srivastava A, Honorato S B, Tandon P, Pessao O D L, Fechine P B A & Ayala A P, *Spectrochim Acta A*, 113 (2013) 367.
34 Xavier R J & Dinesh P, *Spectrochim Acta A*, 118 (2014) 999–1011.
35 Govindarajan M and Karabacak M, *Spectrochim Acta A*, 96 (2012) 421.
36 Glendening E D, Reed A E, Carpenter J E & Weinhold F, NBO Version 31, TCI, University of Wisconsin, Madison, 1998.
37 Andraud C, Brotin T, Garcia C, Pelle F, Goldner P, Bigot B & Collet A, *J Am Chem Soc*, 116 (1994) 2094.
38 Nakano M, Fujita H, Takahata M & Yamaguchi K, *J Am Chem Soc*, 124 (2002) 9648.
39 Geskin V M, Lambert C & Bredas J L, *J Am Chem Soc*, 125 (2003) 15651.
40 Kleinman D A, *Phys Rev*, 126 (1962) 1977.
41 Adant M, Dupuis L & Bredas L, *Int J Quantum Chem*, 56 (1995) 497.
42 Bevan J and Boerio-Goates J, *Calculations from statistical thermodynamics academic press*, (2000).
43 Sajan D, Josepha L, Vijayan N & Karabacak M, *Spectrochim Acta A Mol Biomol Spectrosc*, 81 (2011) 85.
44 Padmanabhan J, Parthasarathi R, Subramaniaan V & Chattaraj P K, *J Phys Chem A*, 111 (2007) 1358–1361.
45 Parr R G, Szentpaly L & Liu S, *J Am Chem Soc*, 121 (1999) 1922.
46 Chattaraj K & Giri S, *J Phys Chem A*, 111 (2007) 11116.